ORNL/TM-6048

Relaxation Behavior of $2\frac{1}{4}$ Cr-1 Mo Steel Under Multiple Loading

R. W. Swindeman
R. L. Klueh

[redacted]

OAK RIDGE NATIONAL LABORATORY
OPERATED BY UNION CARBIDE CORPORATION · FOR THE DEPARTMENT OF ENERGY

Printed in the United States of America. Available from
the Department of Energy,
Technical Information Center
P.O. Box 62, Oak Ridge, Tennessee 37830
Price: Printed Copy $4.50; Microfiche $3.00

ORNL/TM-6048
Distribution
Category
UC-79b, -h, -k

Contract No. W-7405-eng-26

METALS AND CERAMICS DIVISION

RELAXATION BEHAVIOR OF 2 1/4 Cr-1 Mo STEEL UNDER MULTIPLE LOADING

R. W. Swindeman and R. L. Klueh

Date Published - November 1977

OAK RIDGE NATIONAL LABORATORY
Oak Ridge, Tennessee 37830
operated by
UNION CARBIDE CORPORATION
for the
DEPARTMENT OF ENERGY

CONTENTS

RELAXATION BEHAVIOR OF 2 1/4 Cr-1 Mo STEEL UNDER MULTIPLE LOADING*

R. W. Swindeman and R. L. Klueh

ABSTRACT

Multiple-loading relaxation data for annealed 2 1/4 Cr-1 Mo steel are reported for times to 100 hr and for temperatures in the range 450 to 566°C. At 450 and 482°C the relaxation strength rises with the plastic flow stress, and recovery phenomena are not very significant in the time span of concern. At 510, 538, and 566°C the relaxation behavior during the first loading is unusual in the sense that for a period the relaxation rate is almost independent of stress. This behavior is thought to be associated with a strain-induced aging process, which depletes the proeutectoid ferrite of solid-solution strengtheners. At 510°C and above the plastic flow stress partially recovers during the relaxation process. At 566°C there is clear recovery in the sense that the relaxation rates after the first loading depend on the current value of stress and not on history. Multiple loading tests at 566°C on material in the normalized-and-tempered condition show no unusual behavior.

INTRODUCTION

The low-alloy steel 2 1/4 Cr-1 Mo is used extensively in the steam power industry. This material is especially suited for steam generator components, which experience thermal cycling because, relative to austenitic alloys, it possesses a low thermal expansion coefficient, high thermal conductivity, and good resistance to stress-corrosion cracking. The development of mechanical properties data for 2 1/4 Cr-1 Mo steel can be followed in a series of publications produced by the Metal Properties Council.[1,2] Recently, the selection of this alloy as the reference material for the steam generators for the Clinch River Breeder Reactor (CRBR)[3] has produced an expansion of research activities concerned with many aspects of material behavior. The work reported here is concerned with the relaxation behavior in the temperature range 400 to 600°C for

*Work performed under DOE/RDD 189a No. OH048, High-Temperature Structural Design Methods.

times to several hundred hours. This information serves three purposes. First, it checks existing hardening rules, which form an important aspect of the constitutive relations needed for inelastic analysis of high-temperature components.[4] Second, it provides data that can be used in the development of more sophisticated constitutive relations, which embody both hardening and recovery concepts.[5,6] Finally, it provides information about the stability of this alloy with respect to mechanical behavior. This report emphasizes the third purpose. That is, we examine relaxation behavior from a metallurgical viewpoint and consider the implications relative to using such data to develop mechanical models.

The specific material used in this work has been studied by others. Klueh and co-workers[6–9] have described the tensile, creep, and stress-rupture behavior for temperatures to 600°C, while Brinkman and co-workers[10,11] have reported on the low- and high-cycle fatigue behavior in the range 20 to 600°C. Jaske et al.[12] have provided data pertaining to the cyclic hardening and softening, also in the range 20 to 600°C.

MATERIAL AND EXPERIMENTAL TECHNIQUES

The material was obtained from Babcock and Wilcox (Heat 20017) as 25-mm (1-in.) plate, sectioned into pieces about 300 mm (12 in.) square, and annealed as follows: heated to austenitizing temperature (927°C), held for 1 hr, and furnace cooled to 250°C in 27 hr. The resulting microstructure consisted primarily of proeutectoid ferrite with about 5% pearlite and about 1% bainite. The ferrite grain size was in the range ASTM 5–6. Specimens were machined parallel to the rolling direction and conformed to the dimensions shown in Fig. 1. The composition and tensile properties are provided in Tables 1 and 2, respectively.

Most tests were performed in an electrohydraulic testing system using the experimental setup shown schematically in Fig. 2. The extensometer was attached to grooves machined 50 mm apart in the

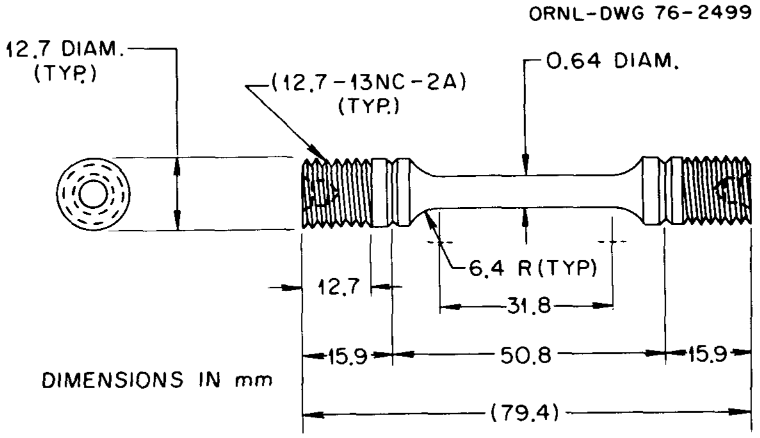

Fig. 1. Relaxation Specimen.

Table 1. Chemical Composition of 25-mm Plate of Annealed 2 1/4 Cr-1 Mo Steel (Heat 20017)

Analysis	Chemical Composition, wt %							
	C	Mn	Si	Cr	Mo	Ni	S	P
Vendor	0.11	0.55	0.29	2.13	0.90		0.014	0.011
ORNL	0.135	0.57	0.37	2.2	0.92	0.16	0.016	0.012

Table 2. Engineering Tensile Properties of Annealed 2 1/4 Cr-1 Mo Steel, $\dot{\varepsilon} = 6.7 \times 10^{-4}/s$

Temperature (°C)	Strength, MPa		Elongation, %	
	0.2% Yield	Ultimate Tensile	Uniform	Total
25	258	525	12.8	28.3
371	227	514	9.5	20.1
454	230	499	8.7	21.0
510	224	459	8.9	23.6
538	217	423	8.4	26.3
566	208	374	7.7	25.9
593	203	328	6.8	36.5

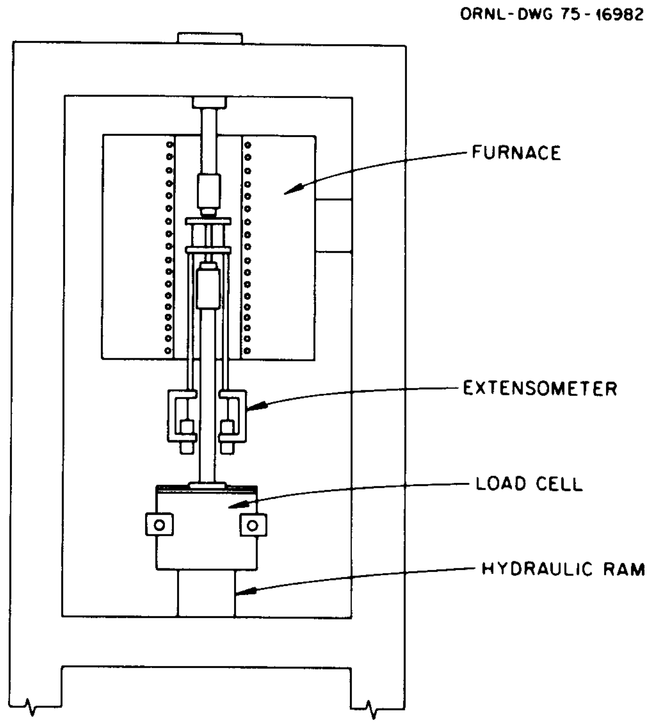

Fig. 2. Schematic of Experimental Setup for Relaxation Testing.

shoulders of the test specimen. This practice resulted in an experimentally measured elastic gage length near 37 mm. In contrast, the plastic gage length was experimentally measured as 32 mm. The extension was sensed by a pair of linear voltage differential transformers, whose output was averaged. The resolution and stability of the extensometer was better than 10^{-5} strain. The heating system consisted of a 410-mm (16-in.) furnace, a 2 kVA power supply, and a two-action D.A.T. controller, which was capable of maintaining temperature within ±2°C of the control point.

Load was monitored by a double-bridge 44-kN (10,000-lb) load cell mounted in series with the specimen. One signal was supplied to a load-extension recorder and the other to a load-time recorder. Tests were performed in a closed loop mode. A command signal, proportional to strain, was fed to a servo-controller, which drove a 44-kN (10,000-lb) hydraulic ram such that the feedback signal from the extensometer matched the command signal. The system was capable of maintaining strain within $\pm 2 \times 10^{-5}$, but in a few instances, specifically in tests at 450 and 482°C, instabilities in the command signal resulted in a temporary change in the strain control point. This produced jumps in strain as great as 10^{-4}. Several longer time tests were performed in an electro-pneumatic system, again in a servo-controlled mode. The test setup and precision were similar to those of the electrohydraulic system described above.

DATA ANALYSIS METHODS

There are several methods for plotting or representing relaxation behavior.[13] Usually, time or log time is taken as the independent variable, while the dependent variable can be stress (σ), fractional stress (σ/σ_0), stress rate ($\dot{\sigma}$), or any of several other indices, which can be considered in either their linear or logarithmic forms. We choose to represent our data by three types of plots. First, we develop an isochronous relaxation curve, similar to that developed from hold-time fatigue data[14,15] and analogous to that developed from constant-load creep data.[16,17] This is a plot of the stress against the applied strain for specific times. The advantage of such a plot is that it enables the veiwer to see the effects of the inelastic strain level on the relaxation strength. Second, we plot stress vs log time, and third, we plot stress vs inelastic strain rate. The inelastic strain rate data are determined by smoothing the stress vs log time plot, reading the time (Δt) required for a stress decrease ($\Delta\sigma$) of 3.45 MPa (500 psi), and converting this to an inelastic strain rate ($\dot{\varepsilon}$) with the known elastic modulus (M). Thus:

$$\dot{\varepsilon} = -\Delta\sigma/M\ \Delta t \ ,$$

where the elastic modulus data are taken from ASME Boiler and Pressure Vessel Code Case 1592. For comparison, stress vs constant-load minimum creep rate curves are constructed for 450, 482, 510, 538, and 566°C by smoothing, interpolating, or extrapolating creep data for the same material.

RESULTS

The isochronous relaxation strength curve constructed from tests on a single specimen at 450°C is shown in Fig. 3(a). The solid line represents plastic flow during loading periods, and the points labeled 1, 2, and 3 represent three relaxation runs performed in the same order. The dashed lines represent the strength curves at 10 and 100 hr. To a first approximation, the relaxation strength curves are parallel to the plastic flow curve. It also appears that relaxation has no significant influence on the subsequent flow stress. Relaxation curves are shown in Fig. 4(a), plotted as stress vs log time. Comparison of run 1, which starts near 234 MPa, with run 2, which starts near 265 MPa, reveals that the relaxation rates are very similar between 0.1 and 100 hr. The curves for all three runs can be superimposed, within the scatter of the data, by a translation paralled to the stress axis. Because of the irregularities in the control point, the variations in

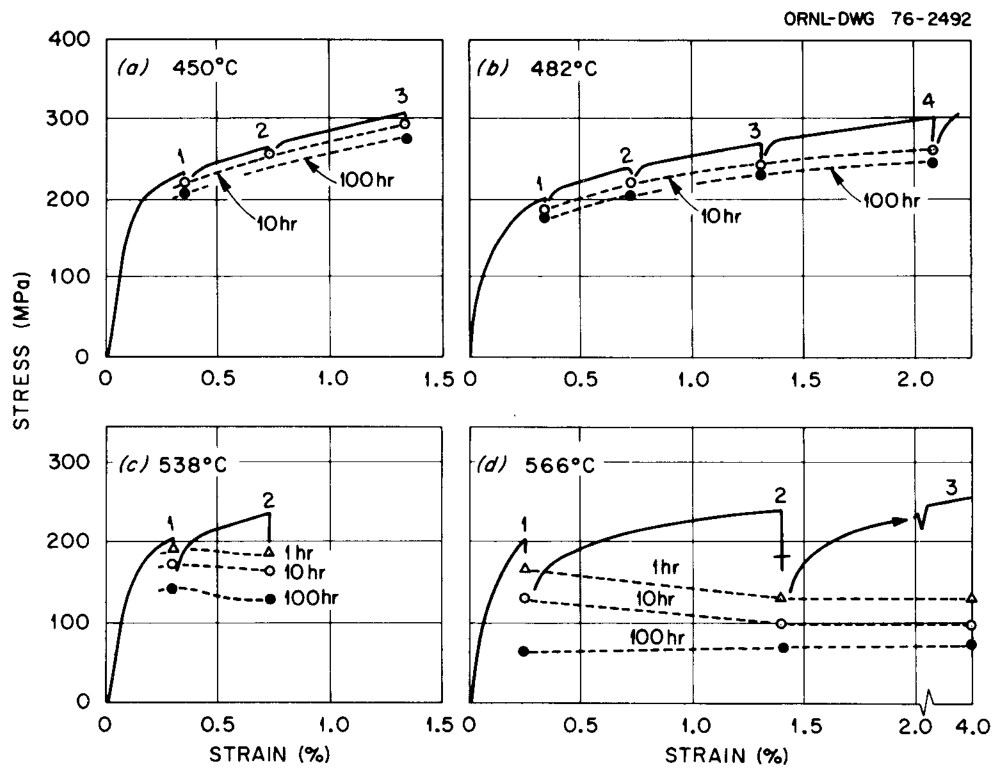

Fig. 3. Isochronous Stress-Strain Curves Obtained from Multiple-Loading Relaxation Tests on Annealed 2 1/4 Cr-1 Mo Steel.

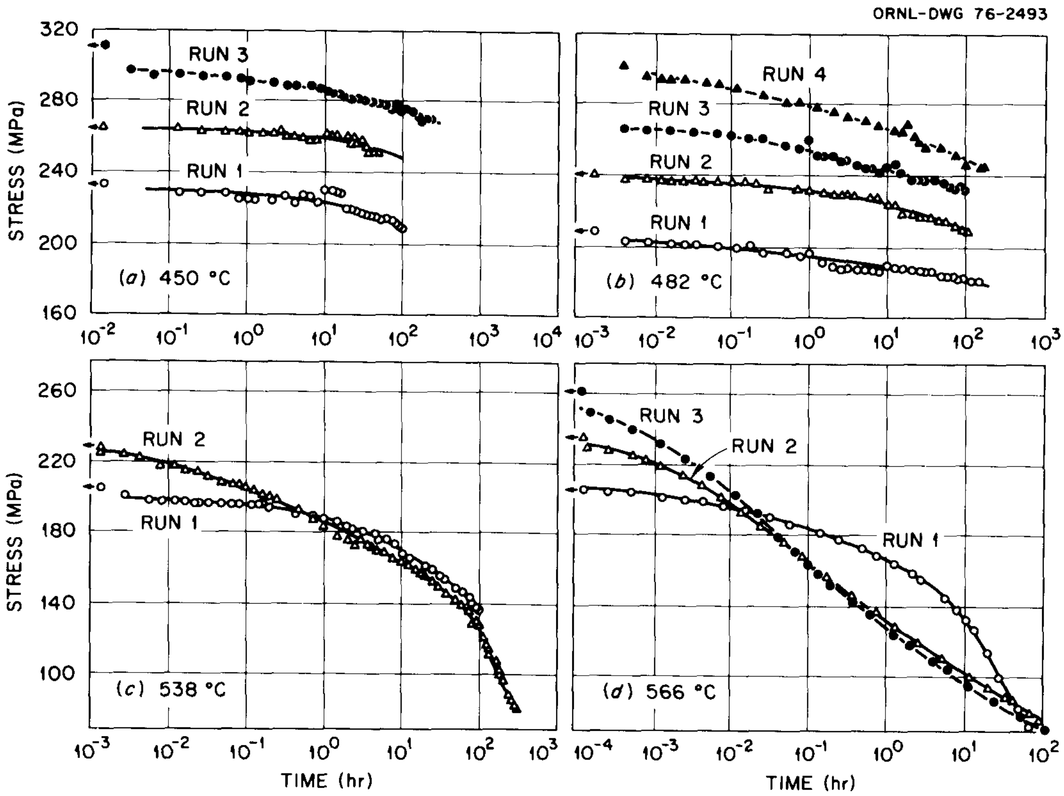

Fig. 4. Relaxation Data Obtained from Multiple-Loading Tests on 2 1/4 Cr-1 Mo Steel at (a) 450°C, (b) 482°C, (c) 538°C, and (d) 566°C.

the stresses are too severe to permit meaningful strain rate data over much of the time period examined. However, some data for runs 1 and 3 are provided in Fig. 5(a), and comparison can be made with constant-load minimum creep rate data included in the figure. Strain rates from run 1 are initially much higher than minimum creep rates, reflecting the fact that primary creep dominates the short-time relaxation behavior. The high-stress strain rates for run 3 are also greater than minimum creep rates at comparable stresses, but eventually the relaxation strain rates diminish to values below the minimum creep rates. The implication of this result will be discussed later in this document.

An isochronous relaxation strength curve at 482°C is shown in Fig. 3(b). Again developed from tests on a single specimen, the curve has features similar to the curve for 450°C. As before, the relaxation strength for any time is roughly parallel to the plastic flow stress,

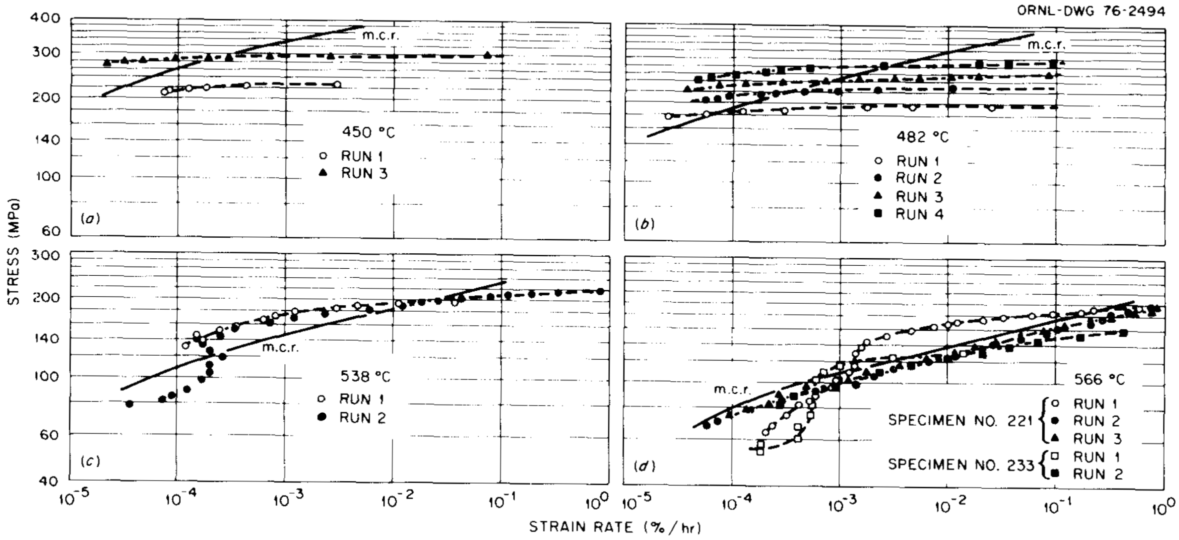

Fig. 5. Comparison of Strain Rates Determined from Relaxation Tests with Minimum Creep Rate Data for Annealed 2 1/4 Cr-1 Mo Steel at (a) 450°C, (b) 482°C, (c) 538°C, and (d) 566°C.

which is not greatly influenced by the relaxation period except after run 4, at the highest strain, where some flow stress is recovered. Relaxation curves for this temperature, shown in Fig. 4(b), exhibit little tendency to converge for at least 100 hr and when strain rate data, calculated from smooth relaxation curves, are compared with minimum creep rate data, as in Fig. 5(b), the data trend is again similar to that at 450°C. Again, the strain rates in relaxation greatly exceed the minimum creep rates at the start of each run and are significantly below the constant-load creep data after 100 hr.

The isochronous relaxation curve obtained from two runs on the same specimen at 538°C is shown in Fig. 3(c). At this temperature we see that the plastic flow stress has partially recovered during the 100-hr relaxation period. Also, the relaxation strength clearly does not parallel the flow curve but might even decrease slightly with increasing strain. Relaxation curves, plotted in Fig. 4(c), reveal a fairly rapid convergence at the high stresses, while, when data are represented in terms of strain rate vs stress as in Fig. 5(c), the strain rates are quite close. Comparison of calculated strain rates with minimum creep rates at the same stress levels reveals an unusual trend. As before, the relaxation rates are initially greater than the minimum values for constant-load tests and drop to rates below the constant-load data. However, as relaxation continues it goes through a period where the strain rate is almost independent of stress, and then decreasing rates are resumed. The net effect is to produce strain rates that, on the average, agree with minimum creep rate data.

The isochronous relaxation strength curve obtained by testing specimen 233 at 566°C is shown in Fig. 3(d). Data in Fig. 3(d) represent three levels of strain: 0.25, 1.4, and 4%, while data (presented later) from another specimen (221) tested at lower strain levels, 0.11, 0.24, and 0.66% indicate the same trend. The plastic flow stress is reduced as a consequence of the 100-hr relaxation period, the short-time relaxation (1 and 10 hr) is more rapid in the second and third runs, and the 100-hr relaxation strength is relatively independent of the strain level for strains greater than 0.2%. Relaxation curves are provided in Fig. 4(d), which shows that the relaxation strength in the second and third runs for specimen 221 falls below the strength in the first run. Strain rate data derived from the relaxation tests is compared with minimum creep rate data in Fig. 5(d). Here the stress vs rate curves for the first run have a sigmoidal shape, which is similar to that observed at 538°C. Strain rates for the second and third runs for specimen 221 do not exhibit this shape but rather appear to be within a factor of 2 of the minimum creep rate. The second run for specimen 233 exhibits a fairly high initial rate, but eventually the data merge with data for specimen 221.

Several relaxation tests were performed at 510°C, although multiple runs were often not included. A series of relaxation curves obtained from single runs on different specimens at this temperature is shown in Fig. 6. In several instances the testing approached 1000 hr. With the exception of the test on specimen 211, which started near 207 MPa, the curves tend to converge near 500 hr. Strain rates calculated from the relaxation tests are compared with minimum creep rate data in Fig. 7(a). For large starting stresses, the relaxation strain rates exhibit the same sigmoidal type of behavior observed at 538 and 566°C. For lower starting stresses, the rates are initially greater than constant-load data but tend toward the minimum creep rate as stresses decrease.

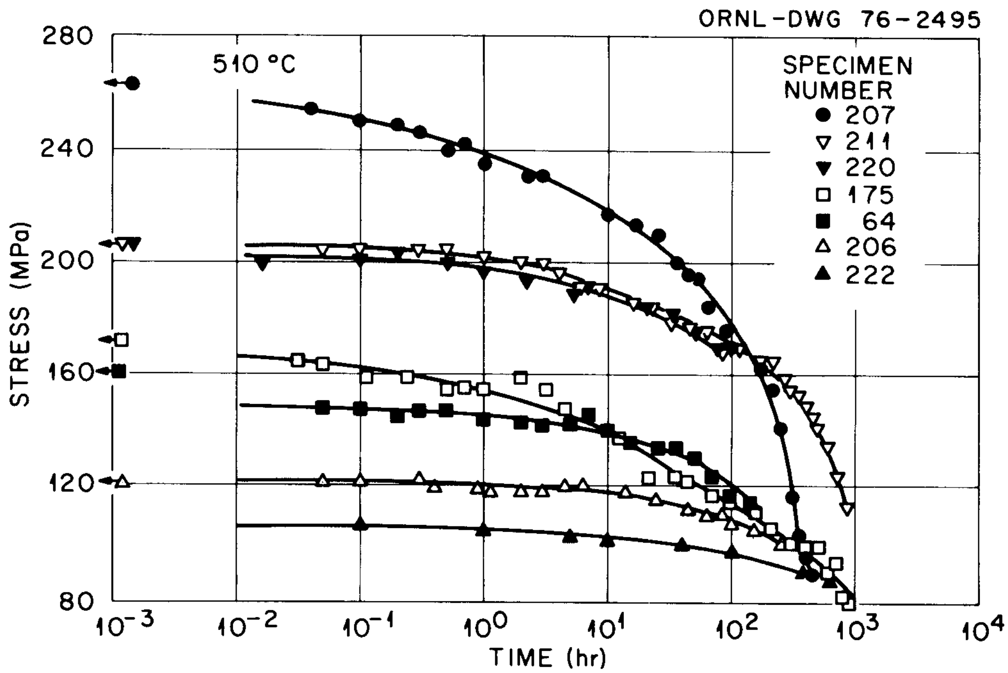

Fig. 6. Relaxation Data Obtained from Single Loadings on 2 1/4 Cr-1 Mo Steel at 510°C.

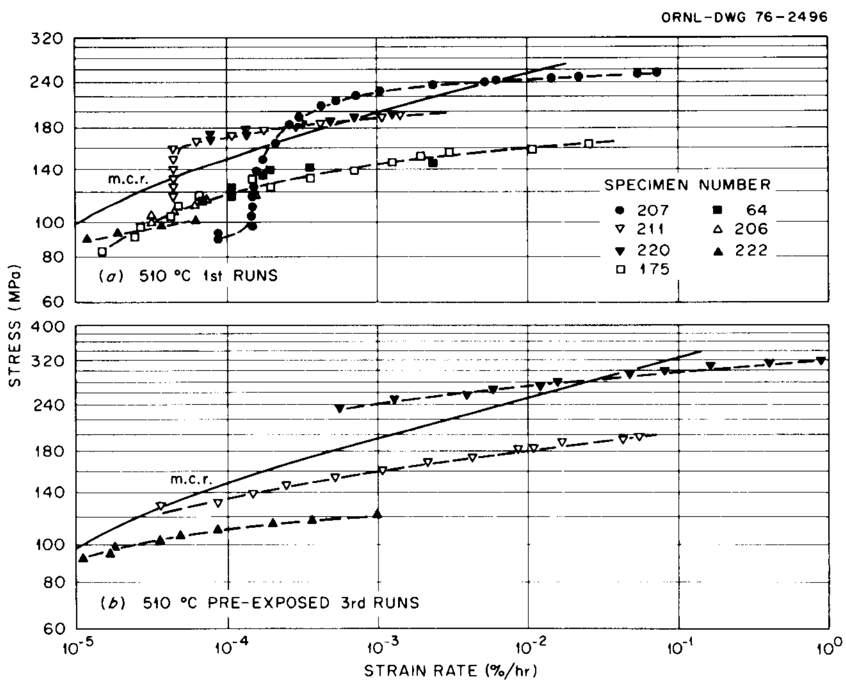

Fig. 7. Strain Rate Data Determined from Relaxation Tests on Annealed 2 1/4 Cr-1 Mo Steel at 510°C.

Strain rate data, obtained from reloaded relaxation tests at 510°C, are shown in Fig. 7(b). The data follow trends similar to data at 450 and 482°C in the sense that the curves shift upward with increased starting stresses and tend to intersect or cross the minimum creep rate curve. All relaxation tests are summarized in Table 3.

Table 3. Summary of Relaxation Data

Specimen	Temperature (°C)	0.2% Yield (MPa)	Strain (%)	Stress, MPa, at Indicated Time in hr						Final Time (hr)	Final Stress (MPa)
				0	0.1	1.0	10	100	1000		
231	450	180	0.350	234	229	227	222	210		100	210
		240	0.735	265	264	263	260			50	252
		270	1.34	310	296	293	286	276		220	270
			1.35	276	279	279	276	267		140	264
177	482	148	0.34	207	200	195	189	181		150	180
		214	0.73	241	236	231	224	208		110	208
		243	1.31	276	261	253	243	232		100	232
		272	2.08	310	290	278	267	250		180	245
			2.0	241	233	227	220			50	210
		307	2.18	308	302	296	283			24	277
		305[a]	2.28	307	294	286	273			24	270
		317	2.4	276	272	266	259			24	250
			2.4	276	272	269	264	252		500	233
222B	510			106	106	105	102	96		600	85
				105	105	103	100	94	72	1000	72
				b	126	124	116	106	87	2000	78
206	510			123	123	120	117	109		260	100
64	510			162	148	145	141	119		150	103
175	510			171	162	155	140	115	81	1000	81
211	510	162	0.25	207	205	202	189	171	100	1000	100
		183	0.43	207	187	167	141			24	138
		207	0.5	207	193	178	155	132		140	128
	566	190	0.56	190	163	136	107	81		150	76
220	510	162	0.25	207	201	200	187	170		100	176
		205	0.31	207	196	188				1	188
		214	b	340	296	267	241			20	233
207	510	b	b	b	252	238	220	172		450	98
176	538	145	0.3	204	195	188	169	137		100	137
		186	0.73	228	206	183	163	129		300	81
233	566	138	0.11	138	133	126	112	54		100	54
		158	0.24	172	145	122	100	72		100	72
		169	0.66	207	151	122	98	78		100	78
	645	b	b	168	103					0.5	90
		b	b	168	103	83	64			20	57
221	566	138	0.25	207	183	166	134	62		100	62
		170	1.4	234	163	131	101	74		100	74
		170	4.0	260	162	127	98	73		200	63

[a]After 70-hr soak at zero strain.

[b]Not recorded.

DISCUSSION AND ANALYSIS

Pugh[4] has developed for this material a creep law, which, when combined with a hardening rule based on creep strain, has made it possible to predict relaxation behavior at 510°C reasonably well. In supplementary studies, Robinson[5] has used variable-load creep data to demonstrate that recovery phenomena are active at 510°C and influence subsequent creep behavior when long rest periods are introduced. This implies that the use of a strain hardening rule could be adequate for single relaxation runs but could underpredict relaxation behavior for multiple loadings. The data that we report here show that a recovery of the plastic flow stress occurs after relaxation periods at temperatures as low as 482°C, but only for very high stresses. The relaxation rate data for the multiple loading situation at 510°C and above suggest that the mechanical behavior is dictated by factors more complex than the competition of strain hardening and time-dependent recovery. Metallurigical factors play an important role. The following discussion outlines some of our current thoughts on this subject.

Both the tensile flow stress[7,8] and the creep strength of annealed 2 1/4 Cr-1 Mo steel depend primarily on the microstructure of the proeutectoid ferrite phase. Klueh[9] has shown that under certain test conditions the creep curves for this material have nonclassical shapes. Instead of the usual single primary, secondary (or minimum creep rate), and tertiary stages, two "minimum creep rate" stages are observed. The transition from the first (Type I) to the second (Type II) involves a quasi-tertiary (increasing creep rate) and a quasi-primary (decreasing creep rate) stage (Fig. 8). The creep rate of the first "minimum creep rate" stage is considerably less than that of the second. The first "minimum creep rate" stage is explained in terms of the interaction solid solution hardening mechanism proposed by Baird and Jamieson[18] for Fe-Mo-C alloys. Strengthening by interaction solid solution hardening results when dislocation motion during creep is restricted by the interaction of molybdenum and carbon atoms or atom clusters with dislocations (i.e., Mo and C form stable units that can interact with dislocations to form atmospheres). With time, the amount of molybdenum

ORNL-DWG 75-14712R2

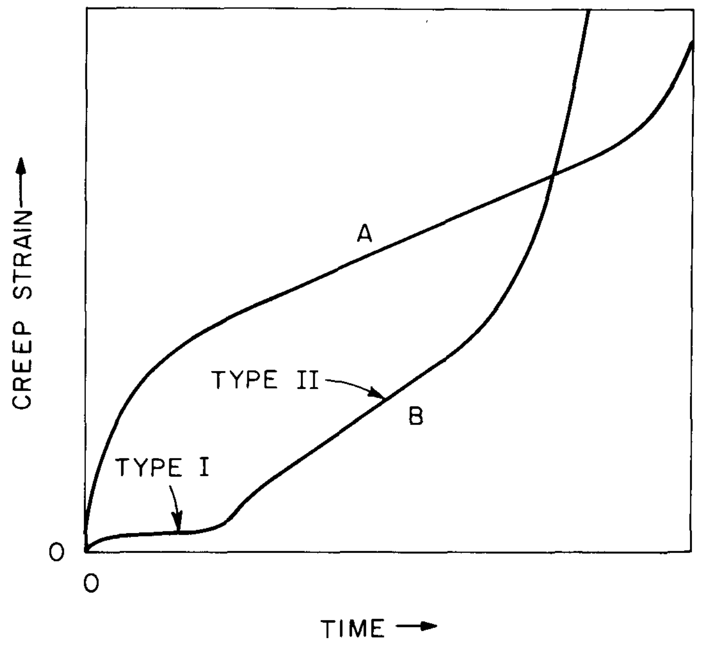

Fig. 8. Schematic Diagrams for Classical (A) and Nonclassical (B) Curves of the Type Observed for 2 1/4 Cr-1 Mo Steel.

and carbon in solid solution decreases until the interaction is no longer effective. At that time the creep rate increases and eventually establishes a new "minimum creep rate" stage. In this new stage the creep rate is controlled by essentially atmosphere-free dislocations moving in the precipitate field of proeutectoid ferrite. The range of temperatures and stresses where this nonclassical behavior occurs is defined in Fig. 9. Clearly, the nonclassical zone covers some conditions where we performed relaxation tests. In comparing relaxation strain rates to creep rates, therefore we have used the values observed in the second "minimum creep rate" stage.

It seems likely that the relaxation process should reflect some of the behavior patterns observed in creep tests. Below 510°C, the precipitation of carbides from the ferrite is sluggish, hence the interaction solid solution hardening phenomenon persists throughout the testing conditions employed in this work. The fact that the relaxation strain rates diminish to values below the constant-load creep rates at equivalent stresses is evidence that time-dependent recovery processes

ORNL-DWG 77-17545

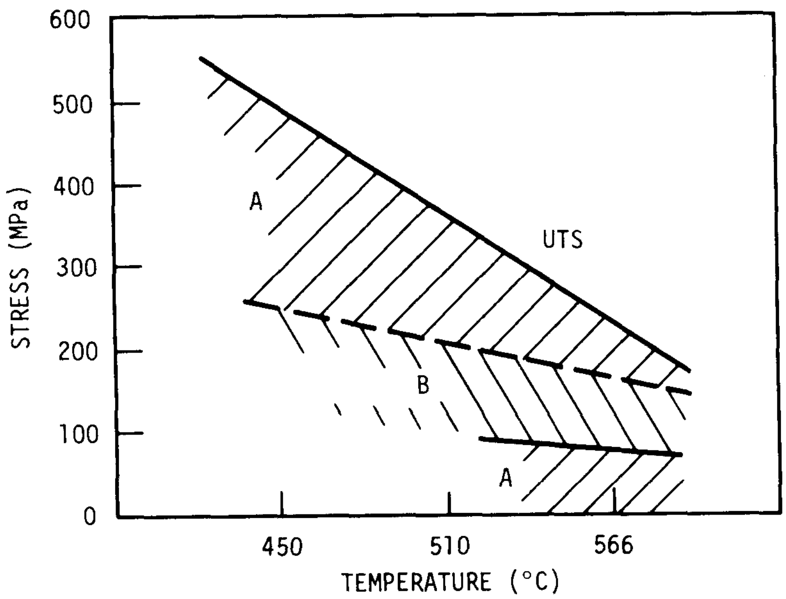

Fig. 9. Region of Stress and Temperature Where Nonclassical Creep is observed in Annealed 2 1/4 Cr-1 Mo Steel.

are extremely slow. Hence, the relation between stress and inelastic strain rate at these temperatures can probably be treated by an approach similar to that used by Hart[19] or outlined by Krausz and Eyring.[20] The Hart approach uses the log stress vs log strain rate curves for different "hardness states" (i.e., different runs) to develop a master curve, which represents rates over a broad range of conditions. Data at 450 and 482°C are not adequate to define the master curve, although simple translations of the curves in log stress vs log rate space will produce coincidence within the data scatter of a single run. In view of the behavior that is observed at temperatures above 482°C, however, it is risky to expect that the annealed material will be metallurgically stable over prolonged times and after many reloadings at the lower temperatures. That is, with the time the molybdenum and carbon are removed from solution by precipitation, and strengthening by interaction solid solution hardening ceases. The log stress vs log strain rate curves at 450 and 482°C would then show, after very long times, the sigmoidal shape observed at the higher temperatures.

At temperatures in the range 510 to 566°C, relaxation testing at high stresses produces a strain-accelerated precipitation of carbides. Although this precipitation could produce a transitional increase in strength, the depletion of carbon and molybdenum from the proeutectoid ferrite matrix minimizes the possibility for long-term interaction solid solution hardening. The higher temperatures also promote higher diffusion rates, which hasten the end of this type of hardening reaction. The shape of the stress vs strain rate curve for the first run probably reflects this microstructural instability.

Initially, the first-run curves exhibit the interaction solid solution strengthening effect, and the lower relaxation rates result from the same processes that lead to the lower creep rate for the first "minimum creep rate" stage during a creep test. With time at this elevated temperature, precipitation lowers the amount of carbon and molybdenum in solution, and interaction solid solution strengthening ceases. Eventually, the relaxation rate approaches the minimum creep rate curve, which is closer to what might be considered as normal (the rate for the second "minimum creep rate" stage in the creep curves[9]).

For 2 1/4 Cr-1 Mo steel, different heat treatments can lead to different relaxation behavior. Klueh has shown that for a tempered bainitic microstructure (the same heat of 2 1/4 Cr-1 Mo steel in the normalized-and-tempered condition) there is considerably less interaction solid solution strengthening.[8,21] Furthermore, creep tests on 2 1/4 Cr-1 Mo steel in this condition displayed classical creep curves.[22]

Several relaxation runs were performed at 566°C using normalized-and-tempered material. Results are plotted in Figs. 10 and 11 and all data, including that from the first run, clearly exhibit a well-behaved trend. The relaxation strain rates shift to lower values after each run, so some degree of strain hardening exists. Relative to minimum creep rate behavior, the relaxation strain rates are much higher at the beginning of each relaxation run. At low stresses the relaxation strain rates merge with or cross the minimum creep rate.

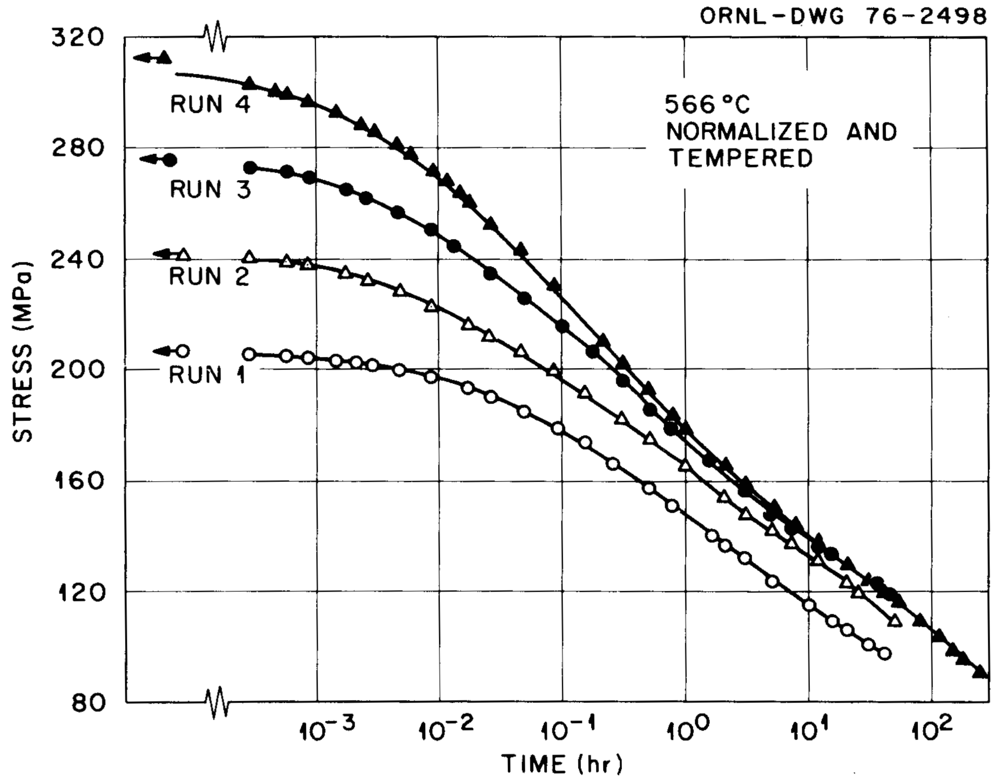

Fig. 10. Relaxation Data Obtained from Multiple-Loading Tests on Normalized-and-Tempered 2 1/4 Cr-1 Mo Steel at 566°C.

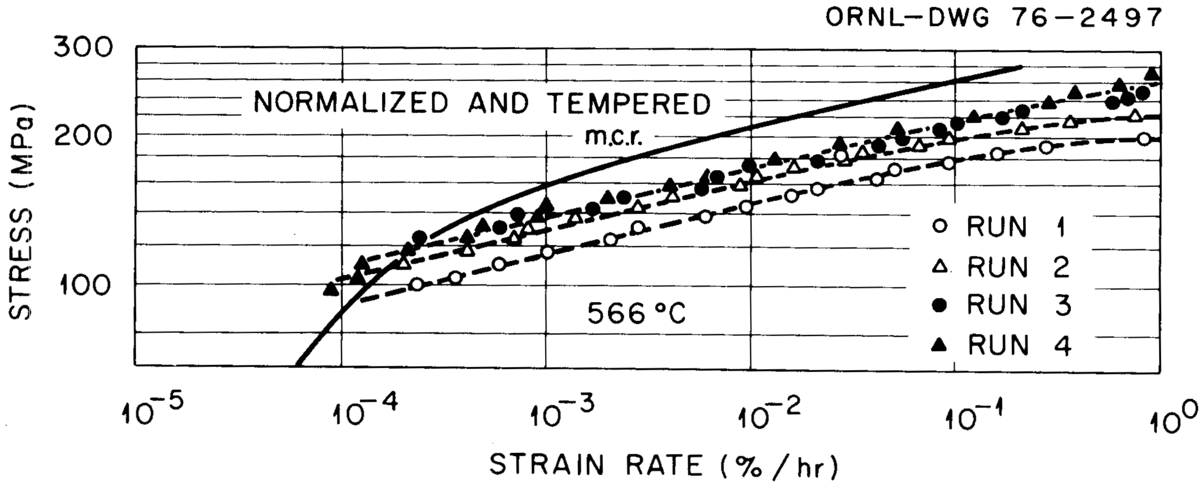

Fig. 11. Creep Rates Determined from Relaxation Data on Normalized-and-Tempered 2 1/4 Cr-1 Mo Steel at 566°C.

This type of relaxation strain rate data could be correlated by translating the curves in log-log space, as was done by Woodford[23] on a Cr-Mo-V steel.

CONCLUSIONS

1. The relaxation strength of annealed 2 1/4 Cr-1 Mo steel under multiple loadings parallels the tensile flow curve at 450 and 482°C for at least 100 hr.

2. At 510°C and above the relaxation behavior in the first loading suggests that a metallurigical instability exists and is manifested by a period during which the relaxation rate is almost independent of stress.

3. At 510°C and above the low-stress relaxation strain rates tend toward the minimum creep rates, determined from constant-load tests at comparable stresses.

4. Normalized and tempered material, tested at 566°C, does not exhibit short-time metallurgical instability. Relaxation rates decrease normally with decreasing stresses and with accumulated strain.

ACKNOWLEDGMENTS

B. C. Williams was responsible for carrying out the experimental work. M. K. Booker and C. E. Pugh assisted in the review and discussion of the material. Sigfred Peterson edited and Gail Golliher prepared the manuscript.

REFERENCES

1. A. O. Schaefer, ed., *Symposium on 2 1/4 Cr-1 Mo Steel in Pressure Vessels and Piping,* G11, American Society of Mechanical Engineers, New York, 1971.

2. A. O. Schaeffer, ed., *2 1/4 Cr-1 Mo Steel in Pressure Vessels and Piping,* G25, American Society of Mechanical Engineers, New York, 1972.

3. J. F. Copland and J. J. Licina, "A Review of 2 1/4 Cr-1 Mo Steel for LMFBR Steam Generator Applications," pp. 55–84 in *Structural Materials for Service at Elevated Temperatures in Nuclear Power Generation*, A. O. Schaeffer, ed., MPC 1, American Society of Mechanical Engineers, New York, 1975.
4. C. E. Pugh, "Constitutive Equations for Creep Analysis of LMFBR Components," pp. 1–15 in *Advances in Design for Elevated Temperature Environment*, S. Y. Zamrik and R. I. Jetter, eds., G00092, American Society of Mechanical Engineers, New York, 1975.
5. D. N. Robinson, *A Candidate Creep-Recovery Model for 2 1/4 Cr-1 Mo Steel and Its Experimental Implementation*, ORNL/TM-5110 (October 1975).
6. R. L. Klueh and T. L. Hebble, "A Mathematical Description for the Stress-Strain Behavior of Annealed 2 1/4 Cr-1 Mo Steel," *J. Press. Vess. Technol.* 98(2): 118–25 (May 1976).
7. R. L. Klueh and R. E. Oakes, Jr., *High-Strain-Rate Tensile Properties of Annealed 2 1/4 Cr-1 Mo Steel*, ORNL/TM-5028, (October 1975).
8. R. L. Klueh, *Heat Treatment Effects on the Tensile Properties of Annealed 2 1/4 Cr-1 Mo Steel*, ORNL-5144 (May 1976).
9. R. L. Klueh, *Creep and Rupture Behavior of Annealed 2 1/4 Cr-1 Mo Steel*, ORNL-5219 (December 1976).
10. C. R. Brinkman, M. K. Booker, J. P. Strizak, and W. R. Corwin, "Elevated Temperature Fatigue Behavior of 2 1/4 Cr-1 Mo Steel," *J. Press. Vess. Technol.* 97: 252–257 (November 1975).
11. C. R. Brinkman, J. P. Strizak, M. K. Booker, and C. E. Jaske, "Time Dependent Strain-Controlled Fatigue Behavior of Annealed 2 1/4 Cr-1 Mo Steel for Use in Nuclear Steam Generator Design," submitted to *Journal of Nuclear Materials*.
12. C. E. Jaske, B. N. Leis, and C. E. Pugh, "Monotonic and Cyclic Stress-Strain Response of Annealed 2 1/4 Cr-1 Mo Steel," pp. 191–212 in *Structural Materials for Service at Elevated Temperatures in Nuclear Power Generation*, A. O. Schaeffer, ed., MPC 1, American Society of Mechanical Engineers, New York, 1975.

13. J. B. Conway, R. H. Stentz, and J. T. Berling, *Fatigue, Tensile, and Relaxation Behavior of Stainless Steels*, TID-26135 (January 1975).

14 W. J. Elder, J. B. Marriott, and M. C. Murphy, "High-Strain Fatigue Properties of Cast 1/2 Cr-Mo-V Steels," pp. 320–31 in *Fatigue at Elevated Temperatures, ASTM Spec. Tech. Publ.* 520, American Society for Testing and Materials, Philadelphia, 1973.

15. J. R. Ellis et al., "Elevated Temperature Fatigue and Creep-Fatigue Properties of Annealed 2 1/4 Cr-1 Mo Steel," pp. 213–246 in *Structural Materials for Service at Elevated Temperatures in Nuclear Power Generation*, A. O. Schaeffer, ed., MPC 1, American Society of Mechanical Engineers, New York, 1975.

16. M. J. Manjoine, "Isochronous Stress-Strain Curves of Type 304 Stainless Steel," *Met. Eng. Quart.* 11(1): 31–3 (1971).

17. A. O. Schaeffer, ed., *The Generation of Isochronous Stress-Strain Curves*, American Society of Mechanical Engineers, New York, 1972.

18. J. D. Baird and A. Jamieson, "Creep Strength of Some Synthesized Iron Alloys Containing Manganese, Molybdenum and Chromium," *J. Iron Steel Inst. London*, 210: 841–46 (1972).

19. E. W. Hart, "A Phenomenological Theory for Plastic Deformation of Polycrystalline Metals," *Acta Metall.* 18(6): 599–610 (June 1970).

20. A. S. Krausz and H. Eyring, *Deformation Kinetics*, Wiley, New York, February 1975, pp. 266–73.

21. R. L. Klueh and R. E. Oakes, Jr. *Strain Rate Effects on the Tensile Properties of a Bainitic (Normalized-and-Tempered 2 1/4 Cr-1 Mo Steel*, ORNL-5134 (April 1976).

22. R. L. Klueh, unpublished research.

23. D. A. Woodford, "Measurement of the Mechanical State of a Low Alloy Steel at Elevated Temperature," *Metall. Trans.* 6A: 1693–97 (September 1975).

ORNL/TM-6048
Distribution
Category
UC-79b, -h, -k

INTERNAL DISTRIBUTION

1–2. Central Research Library
3. Document Reference Section
4–8. Laboratory Records Department
9. Laboratory Records, ORNL RC
10. ORNL Patent Office
11. G. M. Adamson, Jr.
12. R. L. Battiste
13. S. E. Beall
14. R. J. Beaver
15. J. J. Blass
16. M. K. Booker
17. C. R. Brinkman
18. J. P. Callahan
19. D. A. Canonico
20. J. A. Clinard
21–23. J. M. Corum
24. J. E. Cunningham
25. J. H. DeVan
26. T. J. Delph
27. J. R. DiStefano
28. R. Ellis
29. M. H. Fontana
30. W. R. Gall
31. G. M. Goodwin
32. B. L. Greenstreet
33. R. C. Gwaltney
34. W. O. Harms
35. T. L. Hebble
36–38. M. R. Hill
39. D. O. Hobson
40. P. R. Kasten
41. R. T. King
42–44. R. L. Klueh
45. J. M. Leitnaker
46. A. L. Lotts
47. R. E. MacPherson
48. W. R. Martin (Y-12)
49. W. J. McAfee
50. C. J. McHargue
51. L. E. McNeese
52. J. Merkle
53. S. E. Moore
54. P. Patriarca
55. H. Postma
56–58. C. E. Pugh
59. M. Richardson
60. D. N. Robinson
61. W. K. Sartory
62. J. L. Scott
63. V. K. Sikka
64. G. M. Slaughter
65. J. E. Smith
66. J. O. Stiegler
67. J. P. Strizak
68–77. R. W. Swindeman
78. A. T. Trammell
79. D. B. Trauger
80. J. R. Weir, Jr.
81. G. D. Whitman
82. G. T. Yahr
83. T. Yahr
84. R. W. Balluffi (consultant)
85. P. M. Brister (consultant)
86. W. R. Hibbard, Jr. (consultant)
87. Hayne Plamour III (consultant)
88. N. E. Promisel (consultant)
89. D. F. Stein (consultant)

EXTERNAL DISTRIBUTION

90–91. DOE DIVISION OF REACTOR DEVELOPMENT AND DEMONSTRATION, Washington, DC 20545

Director

92–95. ERDA DIVISION OF WASTE MANAGEMENT, PRODUCTION AND REPROCESSING, Washington, DC 20545

Chief, Industrial Programs Branch
Chief, Projects Branch
Chief, Technology Branch

96–97. ERDA OAK RIDGE OPERATIONS OFFICE, P.O. Box E, Oak Ridge, TN 37830

Director, Reactor Division
Director, Research and Technical Support Division

98–361. ERDA TECHNICAL INFORMATION CENTER, Office of Information Services, P.O. Box 62, Oak Ridge, TN 37830

For distribution as shown in TID-4500 Distribution Category, UC-79b (Fuels and Materials Engineering Development); UC-79h (Structural Materials Design Engineering); UC-79k (Components)